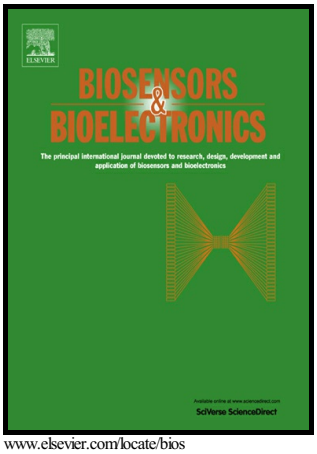

www.elsevier.com/locate/bios

A highly sensitive immunosensor based on ITO thin films covered by a new semi-conductive conjugated polymer for the determination of TNFα in human saliva and serum samples

Elif Burcu Aydın, Muhammet Aydın, Mustafa Kemal Sezgintürk

PII: S0956-5663(17)30374-3
DOI: http://dx.doi.org/10.1016/j.bios.2017.05.056
Reference: BIOS9769

To appear in: *Biosensors and Bioelectronic*

Received date: 20 March 2017
Revised date: 24 May 2017
Accepted date: 31 May 2017

Cite this article as: Elif Burcu Aydın, Muhammet Aydın and Mustafa Kemal Sezgintürk, A highly sensitive immunosensor based on ITO thin films covered by a new semi-conductive conjugated polymer for the determination of TNFα in human saliva and serum samples, *Biosensors and Bioelectronic* http://dx.doi.org/10.1016/j.bios.2017.05.056

A highly sensitive immunosensor based on ITO thin films covered by a new semi-conductive conjugated polymer for the determination of TNFα in human saliva and serum samples

Elif Burcu Aydın[a*], Muhammet Aydın[a], Mustafa Kemal Sezgintürk[b]

[a]Namık Kemal University, Scientific and Technological Research Center, Tekirdağ-TURKEY

[b]Çanakkale Onsekiz Mart University, Faculty of Engineering, Bioengineering Department, Çanakkale-TURKEY

b_e_bahadir@hotmail.com

ebbahadir@nku.edu.tr

[*]Corresponding Author: Tel:+90 282 250 11 37

Abstract

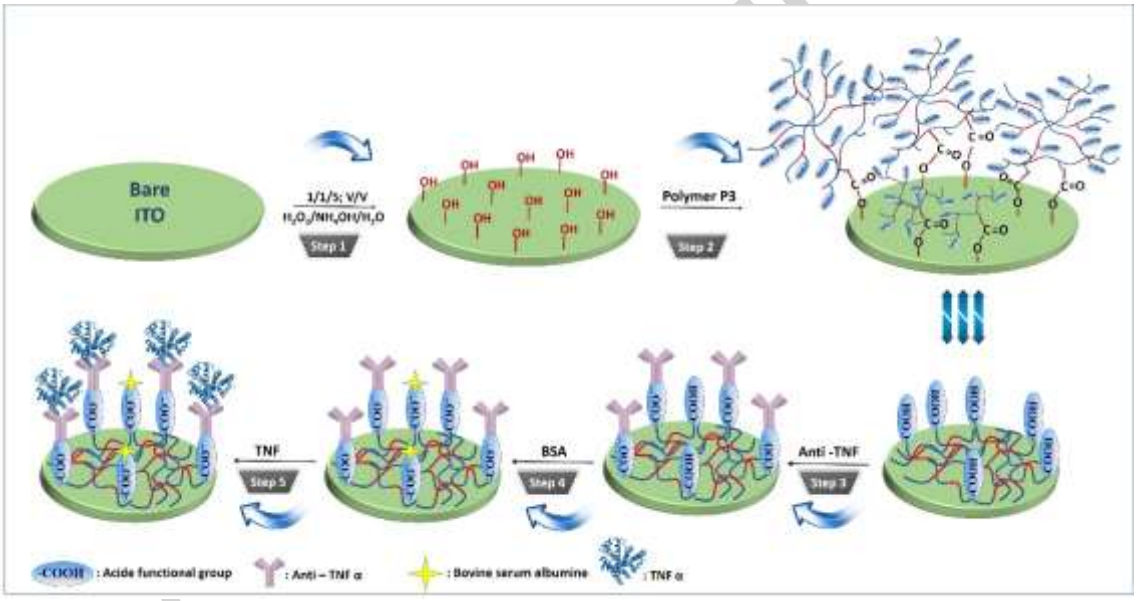

A novel, ultrasensitive impedimetric immunosensor was constructed for the detection of tumor necrosis factor α (TNFα) by using Poly(3-thiophene acetic acid) (P3), a conjugated polymer as an immobilization matrix. The polymer P3 contains a lot of carboxylic acid groups on its surface that provide a larger biorecognition surface. This developed immunosensor was prepared on hydroxy-bearing ITO surface via an ester bond linkage of polymer P3 to immobilize anti-TNF α antibodies. The ITO electrode modification steps and interaction between anti-TNF α antibody and TNF α antigen were monitored by cyclic voltammetry (CV) and by electrochemical impedance spectroscopy (EIS) method. After the analytical parameters optimization, a linear detection response from 0.01 pg/mL to 2

pg/mL, a limit of detection LOD of 3.7 fg/mL and a limit of quantification (LOQ) of 12.4 fg/mL were achieved, which provided accurate results (relative standard deviation; 4.03%). The characterization of this developed immunosensor was performed by using Fourier transform infrared spectroscopy (FTIR), scanning electron microscopy (SEM), SEM-energy dispersive X-ray (EDX) mapping and atomic force microscopy (AFM). The immunosensor allowed a simple and fast detection of TNF α antigen in human serum and satisfied recoveries (98.69-105.20%) were obtained by using standard addition method.

Keywords: Tumor necrosis factor α, label free biosensor, electrochemical impedance spectroscopy, saliva biomarker

1. Introduction

Tumor necrosis factor-α (TNF-α), a 157 amino acid long polypeptide (Liu et al. 2016a), is a pro-inflammatory cytokine secreted by activated macrophages that has a significant role in a wide range of immune and inflammatory processes (Baraket et al. 2014; Baydemir et al. 2016; Kongsuphol et al. 2014). It exists in serum as a biologically active molecule, and its level increases when the inflammatory cascade is activated, that makes TNF-α a very important biomarker for inflammatory based diseases (Baydemir et al. 2016; Kongsuphol et al. 2014). TNF-α is a potential biomarker in different diseases such as rheumatoid arthritis (Baydemir et al. 2016; Eletxigerra et al. 2014; Kongsuphol et al. 2014; Mazloum-Ardakani et al. 2015), neurodegenerative diseases (Alzheimer, Parkinson)(Baydemir et al. 2016; Kongsuphol et al. 2014; Mazloum-Ardakani et al. 2015), diabetes, stroke, HIV infection (Liu et al. 2016a), heart failure (Altintas et al. 2014; Qureshi et al. 2012), lung cancer (Du et al. 2013), colon cancer (Fetahu et al. 2014), leukemia (Zhou et al. 2017), epithelial ovarian cancer (Kolomeyevskaya et al. 2015). Apart from these diseases it has precise role in wound healing (Kolomeyevskaya et al. 2015).

TNF-α is found at very low level in biological samples such as serum. Serum TNF-α concentrations in healthy humans are mostly below 10 pg/mL (Scully et al. 2010), while in more than 80% of patients with severe autoimmune diseases may be in between 10 to 300 pg/mL (Martínez-Borra et al. 2002). TNF-α is also found in saliva, which is a body fluid other than serum (Liu and Duan 2012; Wang et al. 2014). The salivary concentration of TNF α is approximately 30 pg/mL in oral cancer patients and 3 pg/mL in healthy individuals (Liu and Duan 2012). Enzyme-linked immunosorbent assay (ELISA) is the most common technique for the determination of the TNF-α level (Eletxigerra et al. 2014). However, ELISA is expensive, not very reproducible, lacks in standardization, requires a lot time due to multiple assay steps, and large sample volumes are needed. The linear range of ELISA kit is in the range of 0 pg/mL and 800 pg/mL. Many ELISA plates are commercially available, however they have

relatively high background signal owing to non-specific protein adsorption. Other detection methods are radio immunoassays (RIA), bioassays, chemiluminescence imaging, mass spectrometry (MS), immune-PCR, fluorescence immunoassay and electrochemical immunosensor (Bosnjakovic et al. 2012). The TNF α detection methods other than electrochemical immunosensors require expensive devices and skilled personal. Therefore, biosensors have gained attention in recent years due to low cost and user-friendly format.

Recently, there has been increased interest in new bioanalytical techniques such as biosensors and assays for TNF α determination (Baydemir et al. 2016). The usage of TNF α as a biomarker is not widespread in clinic diagnosis and it is used in the field of research area. To overcome these limitations, a wide range of assays and biosensors including optic, piezoelectric, electrochemical measurements have been constructed for the determination of TNF-α (Eletxigerra et al. 2014). These constructed TNF-α biosensors have been developed to simplify the analysis procedure, shorten the analysis duration, increase the detection sensitivity, and decrease the analysis cost (Kongsuphol et al. 2014). For construction of a TNF α biosensor, various type of electrodes such as polyimide substrate (Baraket et al. 2014), screen printed carbon electrode (Eletxigerra et al. 2014), gold electrode (Liu et al. 2013), glassy carbon electrodes have been used (Hou et al. 2013; Li et al. 2012). In this study, we used a disposable and low cost ITO electrode. For the development of the TNF α immunosensor, different nanomaterials such as magnetic microbeads (Eletxigerra et al. 2014), gold nanoparticles (Baraket et al. 2014; Hou et al. 2013; Li et al. 2012), carbon nanotubes (Li et al. 2012) were used. Eletxigerra et al. (2014) reported that microbeads usage increased sensitivity and reduced detection time. They found LOD value as 2 pg/ml. Baraket et al. (2014) and Pui et al. (2012) deposited gold on polyimide substrate and silicon wafer, respectively. Furthermore, they used 16-mercaptohexadecanoic acid and dithiobissuccinimidiyl propionate for SAM formation, respectively. The usage of gold provided low LOD values as 0.1 pg/ml and 1 pg/ml, respectively. Gold was used not only as electrode modification material but also it was used as immobilization material for binding of anti-TNF α antibodies. Hou et al. (2013) prepared hydrogel from ferrocene functionalized phenylalanine and utilized as sensing platform for TNF α detection. TNF α antibodies was immobilized onto electrode via AuNPs. In another study, Li et al. (2012) immobilized TNF α antibodies onto gold nanoparticles modified CNT surface and these antibodies were immobilized on GCE electrode via poly(diallyldimethyl ammonium chloride). The LOD values were 0.5 pg/ml and 2 pg/ml, respectively. It was considered that these low LOD values were orginated from high conductivity of AuNPs and CNT. In our study, we used polymer P3 with numerous carboxyl group for immobilization of anti-TNF α antibodies. These groups increased the amount of binding antibodies and thus a lot of TNF α antigen were captured from TNF α antibodies. Moreover, its semi-conductive property increased sensitivity like other biosensors in which conductive materials were used as interface material.

Electrochemical immunosensor based on electrochemical impedance spectroscopy (EIS) has attracted a lot of attention in biosensor improvement areas (Kongsuphol et al. 2014). EIS is a Faradic impedance method, which is carried out in the presence of a redox couple. It is a label-free technique to determine antigen-antibody interactions on the electrode surfaces by measuring their capacitance and interfacial charge-transfer resistance. EIS technique provides a lot of advantages such as fast analysis and easy detection (Pui et al. 2013).

The design of an electrochemical biosensor requires a chemically modified working electrode. The working electrode is important because its bioreceptor is present on the electrode surface and has a role in the redox reactions which produce a biosensing signal. Indium tin oxide (ITO) is an excellent material, which has been utilized frequently in biosensor studies owing to its unique properties including good optical transparency, wide working window, high electrical conductivity, substrate adhesion and stability (Cheng et al. 2014). Recently, the self-assembled monolayer (SAM) has attracted a lot of interest because SAM formation provides a dense coverage and a closer binding of biorecognition element to the electrode surface. The most studied self-assembled monolayers (SAMs) examples are long-chain functionalized alkanes on gold, alkylsilane derivatives on silica surfaces and alkanoic acids on aluminium oxide and silver. A self-assembled monolayer formation on the ITO surface is an important method which increases the work function of the surface. Organic molecules with end groups of carboxylic acid, phosphonic acid or silane compounds are mostly utilized SAM materials (Wang et al. 2005).

Conducting polymers have attracted a lot of interest due to the excellent physical and chemical features. Conductive polymers have been used in various applications such as rechargeable batteries, sensors, biosensors and drug delivery systems. To obtain sensitive biosensor and analysis at molecular level, the surface of the biosensor is very important. Conducting polymers such as polythiophene (Liu et al. 2015), polyaniline (Chu et al. 2015; Prabhakar et al. 2011), polypyrolle (Liu et al. 2016b) have been utilized as interface material in biosensing systems. Liu et al. (2015) developed a sandwich photeoelectrochemical (PEC) biosensor based on a signal off strategy, the utilized TiO_2 coupled with CdS quantum dots QDs as photoactive matrix and polythiophene made PEC signal stable. Chu et al. (2015) and Prabhakar et al. (2011) electrodeposited polyaniline-gold nanoparticles and polyaniline-stearic acid composite on the ITO electrode surface, respectively. In both studies, polyaniline was used as immobilization matrix for biomolecules.

In the present study, we developed a low-cost and highly sensitive label-free immunosensor based on ITO films coated on a flexible polyethylene terephthalate substrate (PET) to detect TNF-α. To increase the sensitivity of the immunosensor, a conjugated polymer P3 containing carboxyl side groups was synthesized. By using polymer P3 as an immobilization matrix, the surface area of the immunosensor and the active sides for biorecognition element increased. The fabrication steps of ITO electrode included cleaning, activation, ester bond linkage between hydroxyl groups of ITO surface and

carboxyl groups of P3 conducting polymer and activation of polymers -COOH group with 1-ethyl-3-(3-dimethylaminopropyl)carbodiimide (EDC)/N-hydroxysuccinimide (NHS) chemistry and lastly covalent immobilization of antibodies on the electrode surface. The interfacial properties of modified ITO electrode were evaluated by CV and EIS in the presence of $Fe(CN)_6^{4-/3-}$ as the redox active species. Furthermore, the interaction between anti-TNF α antibody and TNF-α antigen was monitored by using single frequency technique (SFI) technique. Apart from these electrochemical methods, SEM, SEM-EDX mapping and AFM were used to identify the morphological features of the surfaces attained after the immobilization stages. Various parameters such as polymer P3 incubation time and concentration, anti-TNF-α incubation time and concentration, TNF-α binding period that effect the fabrication process were optimized. The fabrication and testing of flexible biosensor are described next in a step by step process.

Recent advancements in point-of-care analysis based on cell phone-based technologies, paper-based assays, lab-on-a chip platforms provide monitoring health cost-effectively. They are robust, easy and user-friendly. Our proposed immunosensor offers the advantages such as reduced cost, short analysis time, minimal sample volumes (Vashist et al. 2015). Low-cost materials such as PET films, papers, polymers are a promising platform for developing biosensors. Additional functionality and qualitative analysis can be performed by combining these materials with cell phone. In coming years, we think that, by improving our immunosensor, it can be commercialized to detect wide diagnosis analysis.

2. Experimental

The chemicals and reagents, instruments used, and the synthesis procedure of conjugated polymer P3 and electrode fabrication procedure are explained in the Supplementary information file in detail.

3. Results and Discussion

The monomer and polymers were characterized by FTIR and ^{1}H NMR spectroscopy to show the success of the synthesis method of the monomer and polymers and to determine chemical structure of the polymers and results are displayed in detail in the Supplementary information file.

Figure 1. FTIR spectra of modified polymer P3 electrode (A) and after anti-TNF α immobilization on the ITO electrode (B).

FTIR spectra of polymer P3 layer obtained after formation on ITO surface and immobilization of anti-TNF α antibody on the polymer P3 modified ITO electrode surface are shown in Figure 1. The peak of ester bond between polymer P3 and hydroxyl groups on ITO surface is expected to be observed at around ~1700 cm^{-1}. However, this peak is covered by carbonyl peak of carboxylic acid groups that is found densely on polymer P3. As shown in figure 1A, the strong peak observed at around 1650 cm^{-1} is characteristic of the stretching mode νC=O of the carbonyl involved in carboxylic acid groups on polymer P3. The broad band between 3200 and 3600 cm^{-1} corresponded to the νOH vibration and another band assigned to νC−O−H in plane mode were observed at 1422 cm^{-1} (Arya et al. 2007;

Khaldi et al. 2015). Figure 1B shows the FTIR spectrum of the same surface after anti-TNF α immobilization on ITO electrode. The observation of broad and intense bands for amide I at ~1655 cm^{-1} and for amide II at ~1525 cm^{-1} clearly indicates the presence of the anti-TNF α and polymer P3 (Kong and Yu 2007).

In addition, we examined hydroxylated ITO surface and polymer P3 SAMs formation on hydroxylated ITO surface by using SEM-EDX to evaluate elemental mapping analysis. EDX-mapping images of hydroxylated and polymer P3 modified ITO surface are illustrated in SI-Figs. 3A-B. On EDX-mapping spectra and mapping figure of hydroxylated ITO, oxygen (O), indium (In), and tin (Sn) elements were observed (Figure SI-4). This result is consistent with the literature (Ali et al. 2011). When figure SI-Fig. 1B investigated, EDX-mapping spectra of polymer P3 modified ITO includes carbon (C), oxygen (O), and sulphur (S) elements. This analysis shows that the sulphur atom in thiophene ring of polymer P3 was distributed uniformly on the surface of electrodes, indicating bound polymer P3 on ITO surface. When compared figure SI-Fig 3B to figure SI-Fig 3A, it was monitored that sulphur containing film was formed on the ITO electrode surface and there was not In and Sn elements on the ITO surface. The EDX mapping results was also used to confirm the immobilization of polymer P3 onto the ITO surface.

3.1 Electrochemical detection mechanism of the biosensor

The immunosensor fabrication was performed in four different stages: activation of ITO surface, modification of electrode surface with polymer P3, followed by antibody immobilization and subsequent protein detection, as shown in Scheme 1.

Scheme 1. The bio-functionalization steps of the TNF α biosensor.

The first stage was cleaning of ITO electrode surface. This cleaning procedure is very important to avoid the organic contamination that could adsorb onto ITO surface. Then, the electrodes were hydroxylated by using $NH_4OH/H_2O_2/H_2O$ mixed solution. Covalent attachment of carboxylic acid containing polymer P3 was performed through ester bond formation between the carboxylic acid of polymer P3 and hydroxyl groups of ITO surface and thus a SAM coverage was constructed on the ITO surface (Deng et al. 2014). This ester bond-linkage assembly technique was successful to fabricate the self-assembled polymer based immunosensor. All the immunoreactions were performed on the ITO surface containing activated carboxyl groups. The configuration of the ITO biosensor involved firstly the covalent immobilization of anti-TNF α antibody onto P3 polymer using EDC/NHS chemistry. EDC and NHS acted as a coupling agent and an activator, respectively. After a blockage of the unreacted activated groups of the P3 polymer with BSA, the anti-TNF α antibodies interacted with their TNF α antigens.

EIS and CV were utilized to monitor the electrochemical features of each immobilization step of immunosensor for TNF-α detection. 5 mM ferrocyanide and 5 mM ferricyanide were utilized as a

redox-active probe to observe the electron transfer between the electrolyte and the ITO electrode surface. The modification steps can be easily followed via this redox active probe. Thus, information about these modification steps can be obtained.

EIS is an excellent and ultrasensitive technique to monitor the impedance variation of the biosensor during the modification procedures. This important tool gives information about interfacial features between the electrode surface and electrolyte solution, adsorption process and interactions of biorecognition molecules with electrode surface. The impedance spectra of stepwise fabrication were used in this study are represented in figure 2A. Nyquist plots have a semicircle region at higher frequency related to the electron transfer limited process and a linear straight line at 45^{o} to the real axis at lower frequencies related to the diffusion limited electron transfer process. This Nyquist plot can be modelled by an equivalent circuit (Randles circuit) including the solution resistance (R_s), electron transfer resistance (R_{ct}), Warburg impedance (W) and constant phase element (CPE). (Kumar et al. 2016).

Figure 2. (A) Electrochemical impedance spectra and cyclic voltammograms of TNF α biosensor construction steps.

As seen in figure 2A, significant changes were monitored in the electron transfer resistance during the electrode modification steps. These differences in electron transfer resistance were calculated by using Randles equivalent circuit simulation via Gamry Software (Reference 1000, Gamry Instruments). The semicircle diameter increased slightly after self-assembled monolayer formation on the hydroxylated ITO (ITO/polymer P3). This increment was orginated from self-assembling process. It blocked the electrode surface and obstructed electron transfer. When the increment after conducting polymer P3 SAMs formation was compared to the increment after TESU silane-SAMs formation (Bahadır and Sezgintürk 2016a), there was a big difference. TESU silane SAM modified ITO had bigger R_{ct} than polymer P3 modified ITO due to non-conductive property of TESU silane material. In contrast, polymer P3 is a conducting polymer and increases the sensitivity of immunosensor due to a lot carboxyl groups on its surface. Thus, a lot of biorecognition molecule can be immobilized on the electrode surface. Before the immobilization of biorecognition molecule, this carboxyl groups should be activated. For activation of carboxyl groups, we used EDC/NHS chemistry (ITO/polymer P3/NHS/EDC). As seen in figure 2A, the charge transfer resistance increased due to non-conductive feature of NHS/EDC. As the polymer P3 is negatively charged, the charge repulsion between $[Fe(CN)_6]^{3-/4-}$ and active carboxyl groups reduced the rate of electron transfer. After activation of carboxyl groups, anti-TNF α antibody bound on the ITO electrode surface via amide bonds. Direct and covalent immobilization of anti-TNF α antibody on the ITO surface resulted proper orientation and caused an increase in the semicircle diameter. The remained free reactive sites on the surface after immobilization was then blocked by using BSA (0.5%) for 1 hour. Thus, the semicircle diameter of ITO/polymer P3/anti-TNF α/BSA electrode increased because of the hindrance effect of BSA, that is a

non-conductive molecule. EIS results illustrated us that the construction of immunosensor was performed successfully. At the detection step, the specific interaction occurred between anti-TNF α antibody and TNF α antigen, and an increase was seen in the semicircle diameter due to obstruction of electron transfer.

CV was utilized to monitor the electrochemical features of each immobilization steps of immunosensor for TNF α detection, as illustrated Figure 2B. Curve in Figure 2B showed reversible oxidation and reduction peaks of $[Fe(CN)_6]^{3-/4-}$. The highest oxidation and reduction peak currents on the ITO surface were obtained from hydroxylated ITO electrode. The oxidation and reduction peaks decreased slightly owing to semi-conductive property of polymer P3. After activation of carboxyl group on ITO surface, a decrease was observed in reversible oxidation and reduction peaks owing to the charge repulsion between $[Fe(CN)_6]^{3-/4-}$ and active carboxyl groups of polymer P3. The activated carboxyl groups were covalent binding points for immobilization of biorecognition elements. When the electrode was conjugated with anti-TNF α antibody, the oxidation and reduction peaks reduced, which suggested that the anti-TNF α antibody was successfully immobilized on the electrode surface and formed an additional barrier and it prevented the electron transfer between the redox probe and the electrode surface. Similar result was observed at the oxidation and reduction peaks after BSA and TNF α were immobilized. When these results were evaluated all together, CV results confirmed EIS results.

3.2 Morphology characterization of the biosensor

The modification steps of the biosensor were characterized by SEM and AFM (Figure 3). Figure 3A and 3B show a morphology with a rough and homogenous layer with hydroxyl ends. Hydroxylated ITO includes grains with an area roughness of 4 nm and a root mean squre (rms) roughness of 4.20 nm on a 5 x 5 µm scale. When the polymer P3 covered the hydroxyl groups on the ITO surface, the surface displayed a homogenous film and the morphology of the surface changed due to polymer P3 SAMs formation (Figure 3C and 3D). Polymer P3 modified ITO electrode includes grains with an area roughness of 109.66 nm and an rms roughness of 134.98 nm on a 5 x 5 µm scale. Thus, the surface was an effective matrix for antibody immobilization. Upon the immobilization of antibody, an obvious aggregation of antibodies is shown (figure 3E and 3F), that significantly differed from the data exhibited in figure 3C. Anti-TNF α modified ITO electrode includes grains with an area roughness of 17.70 nm and an rms roughness of 22.30 nm on a 5 x 5 µm scale. BSA is a globular protein. Thus, it had a spherical form on ITO surface (Figure 3G and 3H). BSA modified ITO electrode includes grains with an area roughness of 26.50 nm and an rms roughness of 32.90 nm on a 5 x 5 µm scale. After antibody- antigen interaction the surface morphology was differed. These results demonstrated the successful binding of antigen (Figure 3I). As seen figure 3J, the interaction between anti-TNFα and

and TNF α caused an increase in area roughness. Consequently, the results of SEM experiments proved the accuracy of EIS and CV.

Figure 3. SEM and AFM images of the modification steps occurred on the ITO electrode; hydroxylated ITO (A and B), ITO/polymer P3 (C and D), ITO/polymer P3/anti- TNF α (E and F), ITO/polymer P3/anti-TNF α/BSA (G and H), ITO/polymer P3/anti-TNF α/BSA/TNF α (I and J).

3.3 Optimization of detection conditions

To attain an optimal electrochemical response of the proposed biosensor, the experimental conditions, such as polymer P3 concentration and polymer P3 incubation period, anti-TNF α concentration and anti-TNF α incubation period, TNF α incubation period were optimized.

Using polymer P3 as an interface material did not only improve the conductivity of electrode, but also provided large surface area for immobilization of anti-TNF α antibodies, which increased the sensitivity of fabricated immunosensor. Therefore, polymer P3 concentration and polymer P3 incubation period were optimized. For polymer P3 concentration optimization studies, three different concentration levels (0.5%, 1%, 2%) were studied. The highest response was obtained by using 1% polymer P3 concentration during the experiment. 0.5% polymer P3 concentration usage caused low response because it had less carboxyl group. The increment of polymer P3 concentration increased the electrochemical response. But, 2% polymer P3 concentration usage caused a bit decrease in the response (Figure SI-5). This may be orginated from steric hindrance of carboxyl groups on ITO surface. After optimization of used polymer P3 concentration, polymer P3 incubation time was optimized by using 3 different durations (6 h, 12 h, 24 h). The short incubation time caused a low response because less amount of P3 polymer bound on the hydroxyl groups of ITO electrode. However, longer incubation time caused good signals and similar responses. Therefore, 24 h was chosen as optimum polymer incubation time.

Another optimization steps were antibody concentration and antibody incubation time. The ITO substrates were immersed into anti-TNF α antibody solutions for binding of antibodies onto polymer P3 modified ITO electrodes. For antibody concentration optimization experiment, three different (0.2, 0.4 and 2 ng/mL) antibody concentrations were tried. During the lowest concentration (0.2 ng/mL), low response was obtained, because adequate amount of antibody did not immobilize on the modified ITO surface. The response increased with the increase of antibody concentration and maximum response was obtained during the usage of 0.4 ng/mL antibody. Therefore, the 0.4 ng/mL anti-TNF α concentration was chosen as optimized antibody concentration. The obtained TNF α calibration curves with different amount of anti-TNF α antibody are presented in (Figure SI-6). As seen Fig. 6 (SI), the usage of 0.4 ng/mL anti-TNF α provided high electron transfer resistance and a good linear curve. The antibody incubation time is an important parameter for immobilization of anti-TNF α antibodies on the ITO electrode. For this reason, 3 different incubation durations (30, 45, 60 minutes) were investigated.

Short incubation time of anti-TNF α had low response because sufficient amounts of anti-TNF α was not bound on ITO surface. The other incubation times were enough for binding process and had similar signals, so 45 min was chosen as optimum incubation time (Figure SI-7).

To achieve an optimal electrochemical signal, different antigen incubation times were examined. The incubation time is important to capture antigens on the electrode surface. During this step, recognition events occur and it is the most important step of the fabrication process. Therefore, three different incubation durations (30, 45, 60 min) were studied. The result obtained from 30 min showed that during 30 min, sufficient amounts of TNF α antigens were not bound enough to anti-TNF α antibodies. However, 45 and 60 min incubation times were enough for binding period and maximum response was obtained during 45 min incubation period. Consequently, 45 min was selected as the optimum incubation duration of antibody with antigens. Long incubation time did not improve the response.

3.4 Analytical performances of the immunosensor

Under optimal working conditions the ITO/polymer P3/NHS-EDC/anti-TNF α/BSA biosensor can be employed to detect TNF α sensitively without any label. For quantitative determination of the sensitivity and linear working range of electrochemical immunosensors, the calibration plot of the immunosensor with different concentration of TNF α was drawn by using EIS datas. The EIS response increased with rising concentration of TNF α and showed a wide detection linear range and an excellent linear relationship with the TNF α concentration from 0.01 to 2 pg/mL.

The EIS response, also charge transfer resistance (R_{ct}), were calculated via equivalent circuit model inserted in Figure 2A. This equivalent circuit model includes an ohmic resistance (R_s) corresponding to the resistance of the electrolyte solution, charge transfer resistance (R_{ct}), double layer capacitance related to the capacitance of the complex bioactive layer, and the Warburg impedance (Z_w) related to the normal diffusion to the electrode surface through the complex layer (Bahadır and Sezgintürk 2016a; dos Santos et al. 2015; Karaboğa et al. 2016; Sezgintürk 2011).

When all these informations are taken into consideration, the calibration plot of TNF α biosensor was obtained by using impedimetric results, which were estimated by this equation:

$\Delta R_{ct} = R_{ct}$ (TNF α)-R_{ct} (BSA)

R_{ct}(TNF α) represents the value of the semicirle diameter (charge transfer resistance) after anti- TNF α antibody-TNF α antigen interaction. R_{ct}(BSA) represents the value of the semicircle diameter after BSA immobilization to free carboxyl ends of polymer P3.

Figure 4. Nyquist plots (A) and cyclic voltammograms (C) of the immunosensor incubated in increasing concentrations of TNF α antigen, (B) The calibration curve of the developed immunosensor, (D) SFI spectra obtained from the interaction between anti-TNF α antibody and TNF α antigen.

Figure 4A and 4C illustrates the Nyquist plots and cyclic voltammograms of the immunosensor incubated in increasing concentrations of TNF α antigen, respectively. As seen figure 4A, the increment in the TNF α concentration caused an increment in charge transfer resistance. The linear relationship between ΔR_{ct} and the concentration is illustrated in figure 4B, indicating a wide linear range from 0.01 to 2 pg/mL. The linear regression is given by y= 1381.8x+54.811 with a correlation of R^2=0.998. The lowest concentration detected and quantified are known as limit of detection (LOD) and limit of quantification (LOQ), respectively. LOD, LOQ were calculated by using the equations $3S_{blank}/m$ and $10S_{blank}/m$, respectively (Demirbakan and Sezgintürk 2016). S_{blank} and m illustrate the signal of blank sample and the slope, respectively. By using this equation, LOD and LOQ were calculated as to be 3.7 fg/mL and 12.4 fg/mL, respectively. The low LOD obtained in our work might be attributed to the usage of polymer P3 with large surface area an increase in surface area may cause an increase in the amount of antibody that have bonded on the surface, thus more antibody interacts with its antigen (Aydemir et al. 2016; Bahadır and Sezgintürk 2016b; Park et al. 2016). These results observed that, our developed immunosensor could detect TNF α antigen sensitively. As seen figure 4C, the increment in TNF concentration caused a decrease in oxidation and reduction peak currents. The increment was inversely proportional to the concentration. Because, an increment in the concentration of TNF α on the electrode surface hindered electron transfer. Thus, small peak currents were obtained. Consequently, the gradual increment in TNF α level elicited a gradual decrease in oxidation and reduction peak currents and a gradual increase in electron transfer resistance.

In this study, SFI technique was utilized for characterization of the interaction between anti-TNF α antibody and TNF α antigen. This technique can be used for monitoring the time-dependent changes of an immunosensor surface. The principle of this technique is based on impedance measurements at fixed frequency, so the variations in kinetic parameters are monitored during the measurement. Moreover, SFI measures the impedance at a fixed frequency versus time (Özcan et al. 2014). Therefore, a fixed frequency was chosen as 8 Hz from Bode Plot (Figure SI-8). Fig. 4D displays SFI spectra. During the measurement 0.4 ng/mL anti-TNF α was utilized and the measurement was performed in PBS buffer (pH 7.0). The total measurement time was 45 min. As seen in figure 4D, pink curve is increased in the process of time. This indicated the increased interaction between anti-TNF α antibody and TNF α antigen.

Surface coverage was calculated by using the equilibrium $Q=nFA\Gamma$, where Q is the total charge (C), n the number of electron transferred, F the Faraday constant (96485 C mol^{-1}), A the electroactive surface area (cm^2) and Γ is the surface coverage (mol cm^{-2}) (Suroviec 2012). The surface coverage of hydroxylated ITO electrode was found as 3.45×10^{-8} mol cm^{-2}. After immobilization of polymer 3, an interface material, Γ was found as 3.4×10^{-5} mol cm^{-2}, also this result indicated that surface was increased 1000 fold approximately. After activation of carboxyl groups of polymer P3 with NHS/EDC, the surface coverage was calculated as 3.47×10^{-8} mol cm^{-2}. Thus, much more active

densely packed polymer P3 modified layer was formed on ITO electrode. After immobilization of anti-TNF α antibody (0.4 ng/mL), the surface coverage was calculated as 3.26 x 10^{-8} mol cm^{-2}. As the free active ends bound with BSA (0.5%), that is a globular protein, a large surface area (Γ was found as 3.43 x 10^{-8} mol cm^{-2}) was obtained. In the last step, where TNF α (0,1 pg/mL) biomarker is detected, Γ was found as 3.37 x 10^{-8} mol cm^{-2}. The result showed that there was an antibody-antigen interaction between anti-TNF α antibody and TNF α antigen.

Repeatability and reproducibility are important properties in biosensing technology. For the repeatability test, the equally prepared 20 electrodes were used for detection of 0.1 pg/mL TNF α under the same conditions and the correlation coefficient, average value and standard deviation were calculated as 4.03 %, 0.11 pg/mL, 4.5 pg/mL, respectively. For the reproducibility test, the prepared 80 electrodes were used to draw 10 calibration plots under the same conditions. All of these immunosensors had the same linearity (Figure SI-9C). The relative standard deviations were also estimated by using the slopes of the linear equations of these immunosensors as 2.5%. The obtained results suggested good precision and acceptable reproducibility of the immunosensor.

Storage stability is an important parameter for clinical applicability of any biosensors. To investigate storage stability of the fabricated biosensor, the modified ITO electrodes were stored at 4 ^{o}C (in dry form) for ten weeks. Every week the electrochemical signals were measured. Our immunosensor had good performance during 8 weeks. After 8 weeks, our sensor showed a decrease in impedance values down to 50% of its initial performance (SI figure 9A). This circumstance showed that the immunosensor got damaged. However, our immunosensor revealed the excellent stability.

Reusability is an indicator of a biosensor success. In this test, the robustness of the immunosensor were measured. For the testing of robustness, ITO electrodes were exposed to drastic conditions (alkaline or acidic) after antibody-antigen interactions. Thus, the functional properties of anti-TNF α antibody were measured. In this section, we dipped our ITO substrate in acidic solution (ultra-pure water: HCl, 0.1%) for 5 min. After incubating in PBS solution containing TNF α, we obtained good responses for six cycles and after 6 cycles its surface got damaged (SI figure 9B).

To prove the practicability of the developed immunosensor, the immunosensor employed to detect TNF α in human saliva and serum samples, which were supplied by Namık Kemal University hospital. The saliva and serum samples were diluted 5 and 20 times with PBS solution, respectively. The recovery of TNF α was estimated by standard addition method with adding TNF α to the human saliva and serum samples and the corresponding results are demonstrated in Table 1 (SI). It can be concluded that the immunosensor gives recoveries in the range of 98.39-105.20%, suggesting excellent accuracy of the developed immunosensor. Furthermore, in order to find whether this immunosensor was affected by the presence of common drugs (ampicillin, amoxycillin, erythromycin, clarithromycin, acetylsalicylic acid), proteins (biotin, albumin) and some biomarkers (Sex determining region Y-box 2

(SOX2), Melanoma-associated antigen 1 (MAGE1), Receptor for Activated C Kinase 1 (RACK1), human epidermal growth factor receptor (HER3), vascular endothelial growth factor receptor (VEGFR)) related analysis were performed under the same analysis conditions mentioned before. The response obtained by the addition of potential interferences (10^3 fold higher concentration than TNF α) was much lower than that of the response obtained by the specific binding of TNF α (SI figure 10).

The developed immunosensor was compared with other biosensors reported in literature applied to the TNF α detection and the comparison of biosensors linear ranges and LODs for TNF α is shown in Table 1. As shown in Table 1 (SI), most of the biosensors have very low LOD than the level of TNF α in human serum and saliva. Our developed biosensor had lower detection limit than other biosensors. Lower LOD can be attributed to the conductivity and the large surface area of polymer P3.

The diagnostic determination cost of TNF α is high when ELISA kits are used. In ELISA test, antibodies specific for human TNF α are coated on a plate. The analysis process includes a lot of steps that require a lot of time. The cost of these ELISA kits is approximately 500 $. However, the cost of one ITO based immunosensor is approximately 0.5 $. Furthermore, the preparation of the biosensor is easy, it is reusable and can be prepared by using basic laboratory equipment. The reusability property reduces analysis cost markedly. But ELISA kits are disposable and reusability of this assay is impossible. What is emphasized in this study is the cheapness, high sensitivity, easy miniaturization and portability of the developed biosensor.

4. Conclusion

A new, highly sensitive electrochemical immunosensor was successfully developed for biosensing of TNF α antigen in human serum and saliva samples, using conjugated polymer P3 as an excellent interface material. Polymer P3-based electrode showed large surface area, good conductivity, which is favourable for the effective immobilization of the biorecognition molecules. This study proved that polymer P3 is a promising material for biomolecule immobilization in the development of various types of biosensors. These well designed immunosensor illustrated a low detection limit of 3.7 fg/mL as well as wider linear range from 0.01 to 2 pg/mL and acceptable specificity for TNF α detection. This developed impedimetric immunosensor illustrated excellent analytical performance for the determination of TNF α with high sensitivity, selectivity and good reproducibility. It can be also applied for analysis of TNF α in human serum and saliva samples with satisfactory results. Consequently, this developed biosensor displays that it may serve as a proper diagnostic tool for accurate monitoring of TNF-α. After advancement in biosensor technology, we believe that our sensor can be commercialized to be used in wide diagnosis analysis.

Acknowledgment

The financial support from TÜBİTAK (The Scientific and Technological Research Council of Turkey, Project number: 113 Z 678) is gratefully acknowledged.

5. References

Ali, M., Ibrahim, K., Hamad, O.S., Eisa, M., Faraj, M., Azhari, F., 2011. Rom. J. Phys 56 (5-6), 730-741.

Altintas, Z., Fakanya, W.M., Tothill, I.E., 2014. Talanta 128, 177-186.

Arya, S.K., Prusty, A.K., Singh, S., Solanki, P.R., Pandey, M.K., Datta, M., Malhotra, B.D., 2007. Analytical biochemistry 363 (2), 210-218.

Aydemir, N., Malmström, J., Travas-Sejdic, J., 2016. Physical Chemistry Chemical Physics 18 (12), 8264-8277.

Bahadır, E.B., Sezgintürk, M.K., 2016a. Analyst 141 (19), 5618-5626.

Bahadır, E.B., Sezgintürk, M.K., 2016b. Talanta 148, 427-438.

Baraket, A., Lee, M., Zine, N., Yaakoubi, N., Trivella, M.G., Elaissari, A., Sigaud, M., Jaffrezic-Renault, N., Errachid, A., 2014. Sensors & Transducers 27(5), 15.

Baydemir, G., Bettazzi, F., Palchetti, I., Voccia, D., 2016. Talanta 151, 141-147.

Bosnjakovic, A., Mishra, M.K., Han, H.J., Romero, R., Kannan, R.M., 2012. Analytica chimica acta 720, 118-125.

Cheng, X.R., Hau, B.Y., Endo, T., Kerman, K., 2014. Biosensors and Bioelectronics 53, 513-518.

Chu, W., Zhou, Q., Li, S., Zhao, W., Li, N., Zheng, J., 2015. Applied Surface Science 353, 425-432.

Demirbakan, B., Sezgintürk, M.K., 2016. Journal of Electroanalytical Chemistry 783, 201-207.

Deng, X., Nie, R., Li, A., Wei, H., Zheng, S., Huang, W., Mo, Y., Su, Y., Wang, Q., Li, Y., 2014. Advanced Materials Interfaces 1(7).

Dos Santos, M.B., Azevedo, S., Agusil, J., Prieto-Simón, B., Sporer, C., Torrents, E., Juárez, A., Teixeira, V., Samitier, J., 2015. Bioelectrochemistry 101, 146-152.

Du, Y.-j., Zhang, H.-y., Li, B., Wu, X., Lv, Y.-b., Jin, H.-l., Cao, Y.-x., Sun, J., Luo, Q.-l., Gong, W.-y., 2013. Progress in Neuro-Psychopharmacology and Biological Psychiatry 47, 69-76.

Eletxigerra, U., Martinez-Perdiguero, J., Merino, S., Villalonga, R., Pingarrón, J., Campuzano, S., 2014. Analytica chimica acta 838, 37-44.

Fetahu, I.S., Hummel, D.M., Manhardt, T., Aggarwal, A., Baumgartner-Parzer, S., Kállay, E., 2014. The Journal of steroid biochemistry and molecular biology 144, 228-231.

Hou, Y., Li, T., Huang, H., Quan, H., Miao, X., Yang, M., 2013. Sensors and Actuators B: Chemical 182, 605-609.

Karaboğa, M.N.S., Şimşek, Ç.S., Sezgintürk, M.K., 2016. Biosensors and Bioelectronics 84, 22-29.

Khaldi, K., Sam, S., Gouget-Laemmel, A., Henry de Villeneuve, C., Moraillon, A., Ozanam, F., Yang, J., Kermad, A., Ghellai, N., Gabouze, N., 2015. Langmuir 31(30), 8421-8428.

Kolomeyevskaya, N., Eng, K.H., Khan, A.N.H., Grzankowski, K.S., Singel, K.L., Moysich, K., Segal, B.H., 2015. Gynecologic oncology 138 (2), 352-357.

Kong, J., Yu, S., 2007. Acta biochimica et biophysica Sinica 39 (8), 549-559.

Kongsuphol, P., Ng, H.H., Pursey, J.P., Arya, S.K., Wong, C.C., Stulz, E., Park, M.K., 2014. Biosensors and Bioelectronics 61, 274-279.

Kumar, S., Kumar, S., Tiwari, S., Augustine, S., Srivastava, S., Yadav, B.K., Malhotra, B.D., 2016. Sensors and Actuators B: Chemical 235, 1-10.

Li, T., Si, Z., Hu, L., Qi, H., Yang, M., 2012. Sensors and Actuators B: Chemical 171, 1060-1065.

Liu, J., Duan, Y., 2012. Oral oncology 48 (7), 569-577.

Liu, L., Liu, F., Jiang, D., Xiang, G., Liu, C., Yang, J., Pu, X., 2016a. Sensors and Actuators B: Chemical 231, 680-687.

Liu, Y., Li, R., Gao, P., Zhang, Y., Ma, H., Yang, J., Du, B., Wei, Q., 2015. Biosensors and Bioelectronics 65, 97-102.

Liu, Y., Ma, H., Zhang, Y., Pang, X., Fan, D., Wu, D., Wei, Q., 2016b. Biosensors and Bioelectronics 86, 439-445.

Liu, Y., Zhou, Q., Revzin, A., 2013. Analyst 138 (15), 4321-4326.

Martínez-Borra, J., López-Larrea, C., González, S., Fuentes, D., Dieguez, A., Deschamps, E.M., Pérez-Pariente, J.M., López-Vázquez, A., de Francisco, R., Rodrigo, L., 2002. The American Journal of Gastroenterology 97, 2350-2356.

Mazloum-Ardakani, M., Hosseinzadeh, L., Khoshroo, A., 2015. Journal of Electroanalytical Chemistry 757, 58-64.

Özcan, B., Demirbakan, B., Yeşiller, G., Sezgintürk, M.K., 2014. Talanta 125, 7-13.
Suroviec, A.H., 2012. Chem. Educator 17, 83–85.
Park, C.S., Lee, C., Kwon, O.S., 2016Polymers 8 (7), 249.
Prabhakar, N., Matharu, Z., Malhotra, B., 2011. Biosensors and Bioelectronics 26 (10), 4006-4011.
Pui, T.S., Kongsuphol, P., Arya, S.K., Bansal, T., 2013. Sensors and Actuators B: Chemical 181, 494-500.
Qureshi, A., Gurbuz, Y., Niazi, J.H., 2012. Sensors and Actuators B: Chemical 171, 62-76.
Scully, P., McKernan, D.P., Keohane, J., Groeger, D., Shanahan, F., Dinan, T.G., Quigley, E.M., 2010. The American Journal of Gastroenterology 105, 2235-2243.
Sezgintürk, M.K., 2011. Biosensors and Bioelectronics 26(10), 4032-4039.
Vashist, S.K., Luppa, P.B., Yeo, L.Y., Ozcan, A., Luong, J.H., 2015. Trends in biotechnology 33 (11), 692-705.
Wang, S., Han, X., Hu, X., Wang, X., Zhao, L., Tang, L., Feng, Y., Wu, D., Sun, Y., Shi, Y., 2014. Clinica Chimica Acta 430, 63-70.
Wang, W., Zhai, J., Jiang, L., Bai, F., Ren, Y., Zhang, B., Cai, S., 2005. Colloids and Surfaces A: Physicochemical and Engineering Aspects 257, 489-495.
Zhou, X., Li, Z., Zhou, J., 2017. Experimental Hematology 45, 17-26.

Highlights

- A low cost, sensitive and disposable immunosensor was developed for TNF α detection.
- The immunosensor was characterized by cyclic voltammetry (CV), electrical impedance spectroscopy (EIS), fourier transform infrared spectroscopy (FTIR), scanning electron microscopy (SEM) and atomic force microscopy (AFM).
- To improve the sensitivity of the immunosensor, polymer P3, a semi-conductive and conjugate material, was used.
- The detection limit and detection range were 3.7 fg/mL and 12.4 fg/mL, respectively.
- The developed immunosensor illustrated good repeatability, stability and selectivity for TNF α detection.

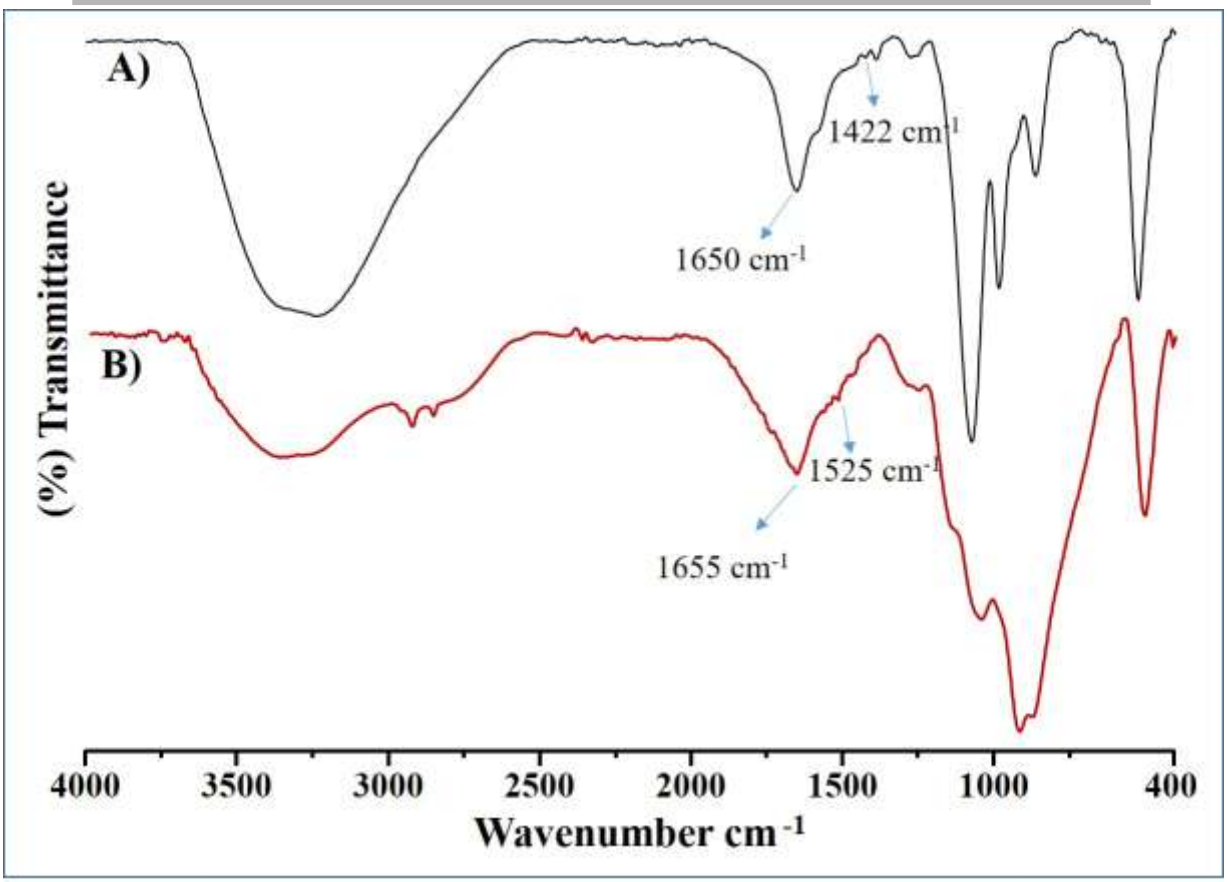

Fig 1

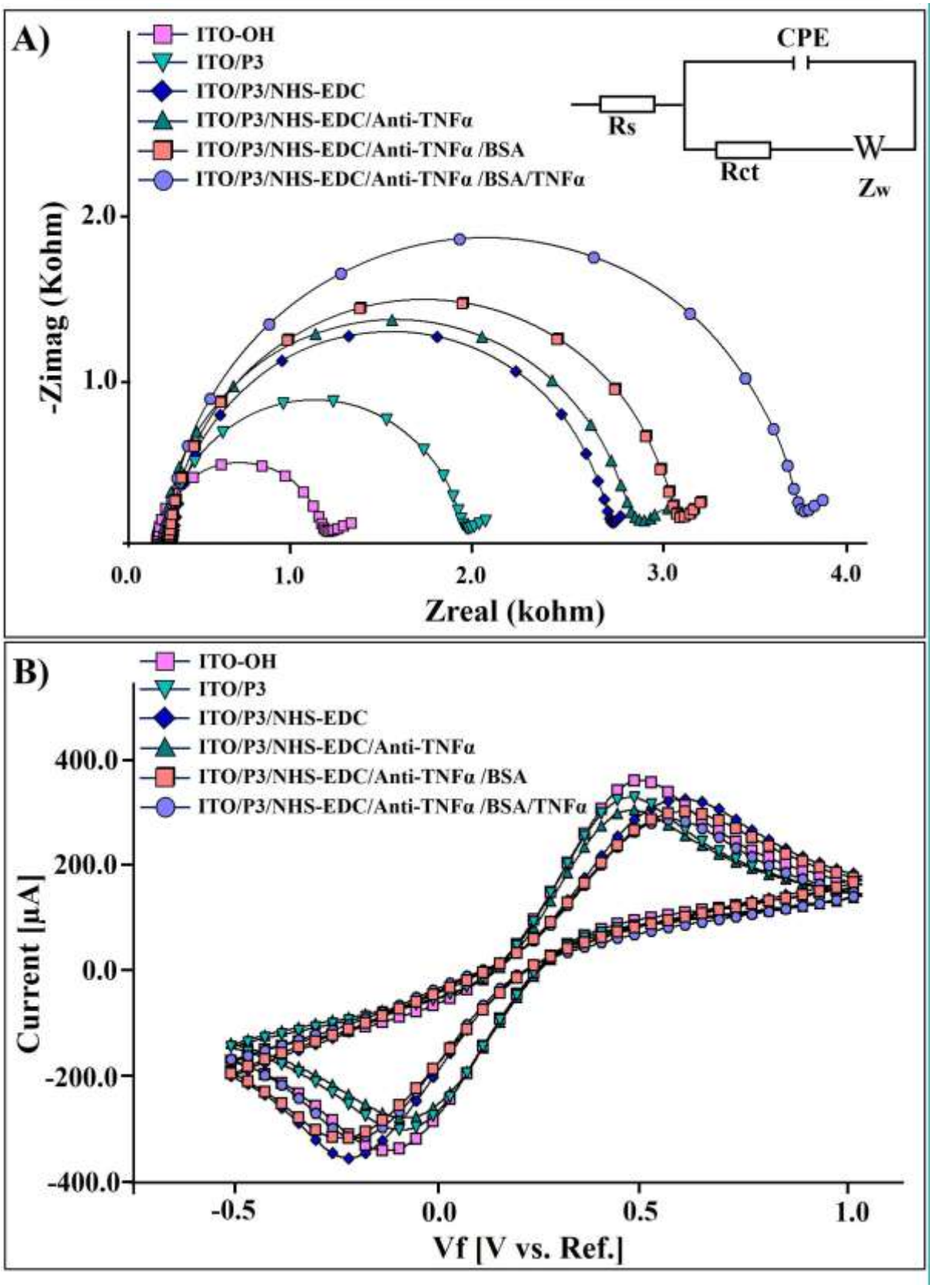
A)
ITO-OH
ITO/P3
ITO/P3/NHS-EDC
ITO/P3/NHS-EDC/Anti-TNFα
ITO/P3/NHS-EDC/Anti-TNFα /BSA
ITO/P3/NHS-EDC/Anti-TNFα /BSA/TNFα
CPE
Rs
Rct
W
Zw
-Zimag (Kohm)
2.0
1.0
0.0
1.0
2.0
3.0
4.0
Zreal (kohm)
B)
ITO-OH
ITO/P3
ITO/P3/NHS-EDC
ITO/P3/NHS-EDC/Anti-TNFα
ITO/P3/NHS-EDC/Anti-TNFα /BSA
ITO/P3/NHS-EDC/Anti-TNFα /BSA/TNFα
400.0
200.0
0.0
-200.0
-400.0
Current [μA]
-0.5
0.0
0.5
1.0
Vf [V vs. Ref.]

Fig 2

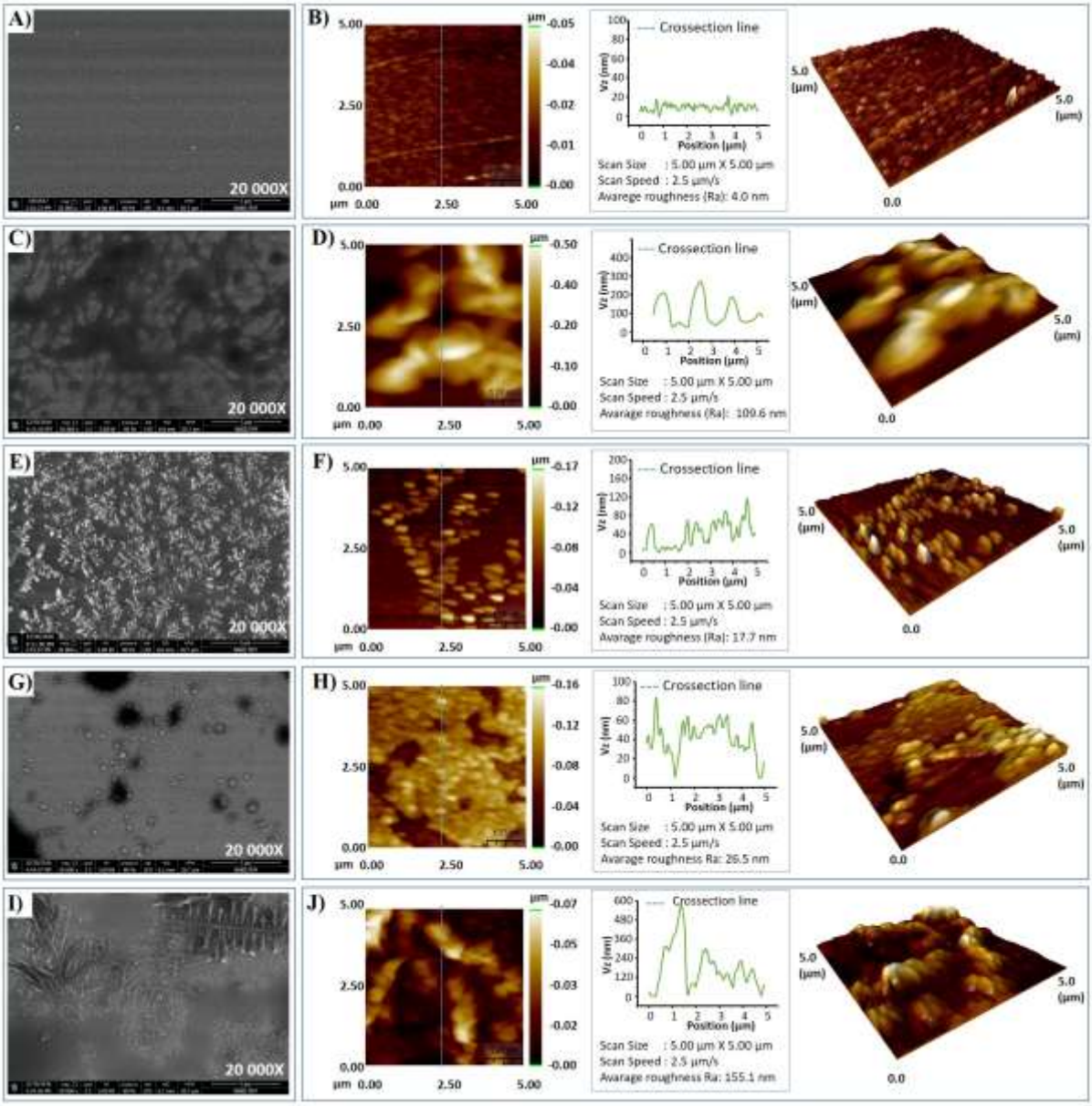
A)
20 000X
B)
Crossection line
Scan Size : 5.00 µm X 5.00 µm
Scan Speed : 2.5 µm/s
Avarege roughness (Ra): 4.0 nm
C)
20 000X
D)
Crossection line
Scan Size : 5.00 µm X 5.00 µm
Scan Speed : 2.5 µm/s
Avarage roughness (Ra): 109.6 nm
E)
20 000X
F)
Crossection line
Scan Size : 5.00 µm X 5.00 µm
Scan Speed : 2.5 µm/s
Avarage roughness (Ra): 17.7 nm
G)
20 000X
H)
Crossection line
Scan Size : 5.00 µm X 5.00 µm
Scan Speed : 2.5 µm/s
Avarage roughness Ra: 26.5 nm
I)
20 000X
J)
Crossection line
Scan Size : 5.00 µm X 5.00 µm
Scan Speed : 2.5 µm/s
Avarage roughness Ra: 155.1 nm
Position (µm)

Fig 3

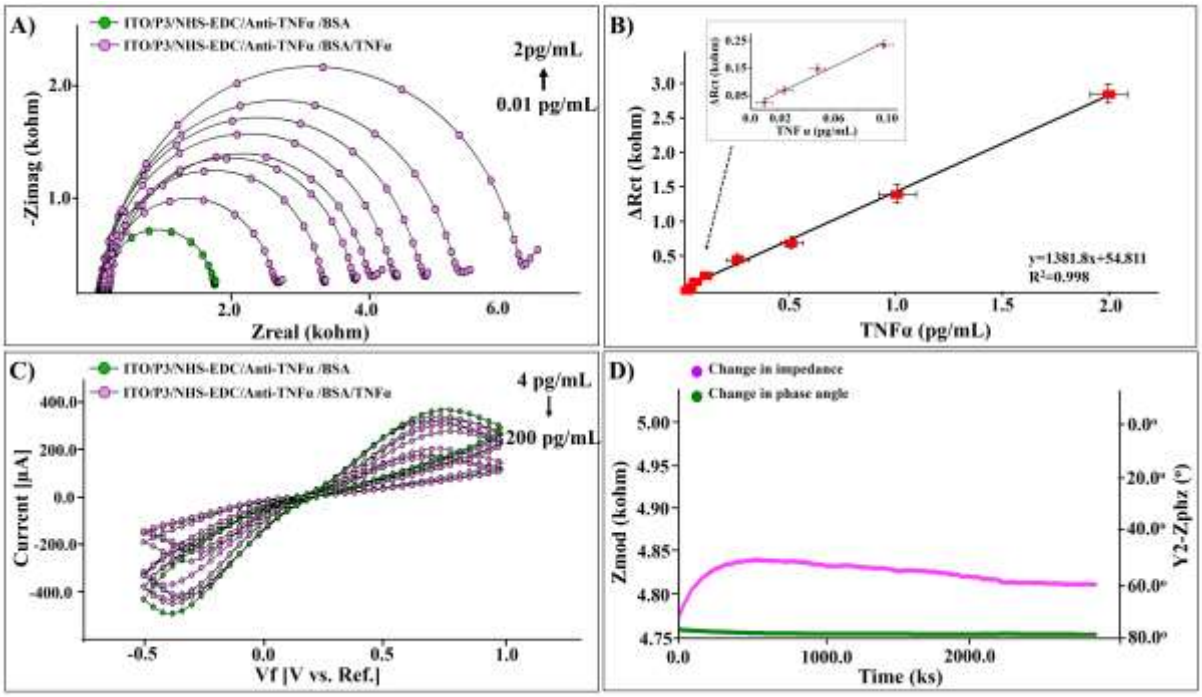

Fig 4

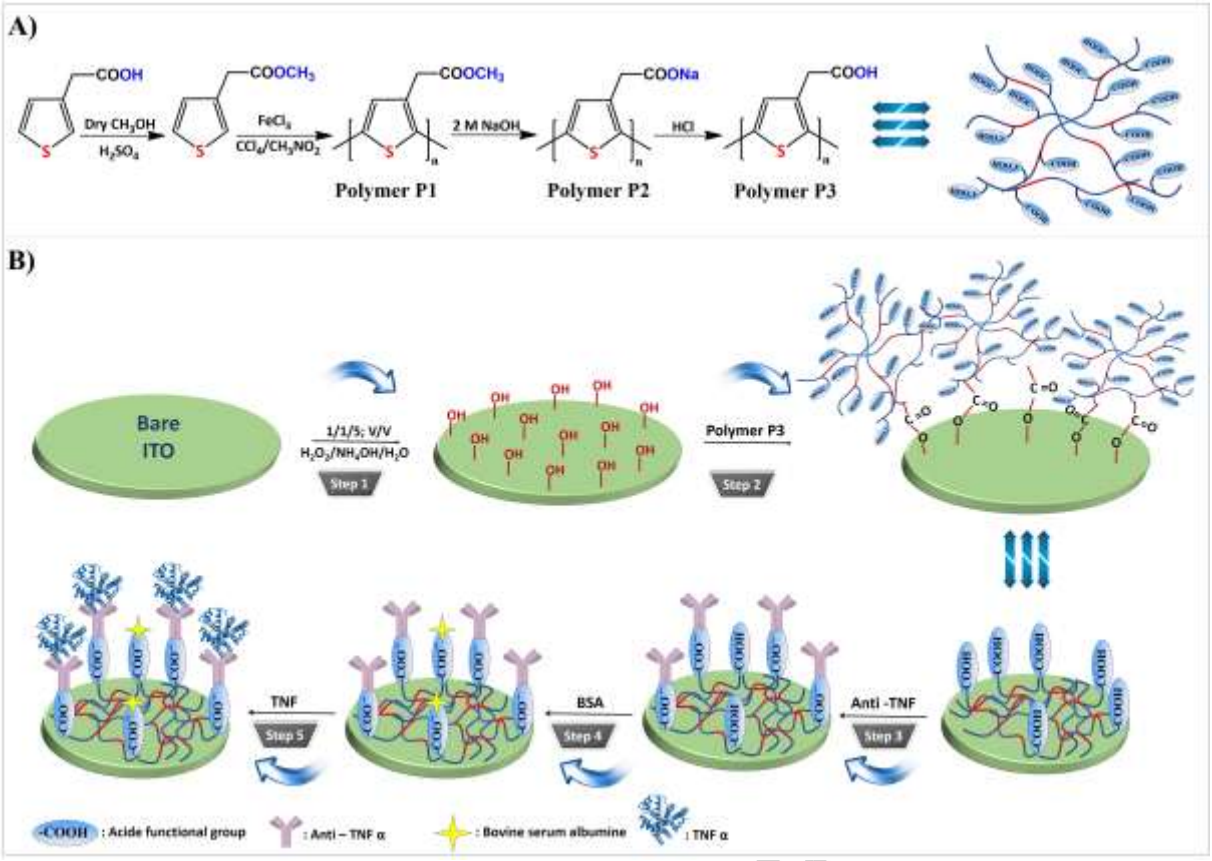

Scheme 1